The 11th Canadian Conference on Earthquake Engineering
Canadian Association for Earthquake Engineering

SAFE, AN EXPERIMENTAL EVIDENCE OF THE FREQUENCY DEPENDENCE OF SHEAR WALL SEISMIC DESIGN MARGINS

Pierre LABBE
EDF, Nuclear Engineering Division, France
pierre.labbe@edf.fr

ABSTRACT: The SAFE experimental programme consists of a series of 10 specimens of shear walls, with different reinforcement ratios, tested until their ultimate capacity under seismic input motion by the pseudo dynamic method. A unique input signal is used, calibrated for controlling the seismic demand. Its input central frequency is selected so that for some specimens it is lower than their eignenfrequency, while for other ones it is the opposite. In conclusion there is clear experimental evidence that design margins are much larger in the second case (input central frequency larger than structure eignenfrequency) than in the first one.

1. Purpose of the SAFE Programme

Because the vast majority of nuclear buildings are made of shear walls, the Kashiwasaki-Kariwa (2007) and the Fukushima (2011) seismic events, have renewed the interest for realistic estimates of shear wall actual capacities, or in other words of their design margins. Although it was launched in the nineties, the SAFE research programme intended actually to provide data on such margins, and more precisely to provide experimental evidences that the frequency content of the seismic input motion plays a crucial role when estimating the actual seismic capacity of shear wall buildings. The SAFE programme was co-funded by Electricité de France (EDF), the Compagnie Générale des Matières Nucléaires (COGEMA, now part of AREVA) and the European Commission Joint Research Centre (JRC), Ispra, Italy.

The testing campaign, designed by Gallois (1994), was performed by the European Laboratory for Structural Assessment (ELSA) of the JRC (Pégon 1999). The JRC uses the pseudo-dynamic test method, which consists of applying displacements on the structure through actuators attached on a reaction wall. The method combines numerical integration of the dynamic equilibrium equation of the system (to compute the displacement to be applied) with measurement of reaction forces corresponding to the prescribed displacement. The measured restoring forces are used to feed the said equation of motion back. The dynamic equilibrium equation does not include a damping matrix (Molina et al., 2011).

Several authors published theoretical research covering a reduced part of the SAFE programme (Mazars et al., 2002; Kotronis et al., 2003; Brun et al., 2003 and 2011; Gallitre, 2008). A recent paper by Labbé et al. (2015), summarized here, presents the full set of SAFE experimental inputs and outputs.

Test of nuclear type shear walls were also carried out from 1994 to 2003, by the Japan Nuclear Energy Safety Organisation (Kitada et al. 2006). The main conclusion was that methodologies presented in JEAG-4601 (NRC 1994) were validated, including an analytical methodology applicable in the range equal to or less than 2 × 10–3 rad. An equivalent viscous damping was identified. Series of tests of shear walls were also performed in USA, in particular at Los Alamos National Laboratory, summarized by the IAEA (2011). A database of more than 400 walls was processed by by Gulec & Whittaker (2009) to obtain a performance based assessment of squat shear wall. In Europe, a database of more than 600 walls, a small minority of them being squat, has been gathered by the Patras University (Grammatikou et al. 2014).

2. The SAFE program

2.1. SAFE concept and implementation

The SAFE experimental programme consisted of a series of specimens of shear walls, with different reinforcement ratios, tested under seismic input motion until their ultimate capacity. The concept is schemed in the Figure 1. The wall is clamped at the base on a rigid body and equipped at the top with a rigid mass, M1, in such a way that it constitutes a single degree of freedom (SDOF) dynamic system in shear. An additional mass M2, acting only in the horizontal direction, is calibrated so that the theoretical natural frequency takes one of the following values: 4 Hz, 8 Hz or 12 Hz.

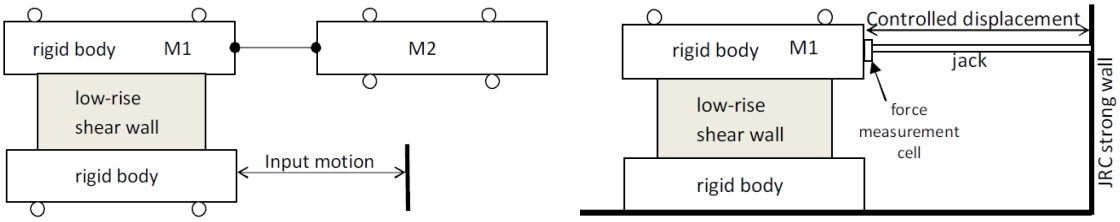

Figure 1 - SAFE conceptual design (left) and conceptual implementation at the JRC Ispra (right)

A unique seismic input signal is used for the whole campaign. For every specimen the signal is first calibrated so that it is just acceptable according to the nuclear industry rules. Then the margin is derived from a series of runs, carried out with increasing input levels until the ultimate wall capacity is observed. The input motion is such that for some specimens its central frequency is lower than the specimen eigenfrequency (low-frequency input) while for other ones it is the opposite (high-frequency input). The SAFE objective is to provide evidence of the frequency dependence of the seismic design margin.

The SAFE conceptual design cannot be implemented on a shaking table because either M2 is from far too large (hundreds of tons) or it would result in a too small scale mock-up. In the pseudo-dynamic method available at the JRC Ispra, M2 becomes a virtual mass, numerically represented in the computer. Concurrently the specimen is clamped on the strong floor and the input motion is replaced by a horizontal force applied at the top, as also presented in the Figure 1. The test is conducted so as to induce the same response of the wall as it would have been under the requested seismic input motion. In practice the test is displacement-controlled and the applied force is measured.

The useful part of the SAFE campaign consisted of 10 specimens numbered T3 to T12. T1 and T2 were used to set-up and calibrate the continuous pseudo dynamic method (Pégon 1999, Pégon et al. 2008).

2.2. SAFE specimens

The core of every SAFE specimen is a shear wall of length L=3 m, height H=1.2 m and thickness ti=16 cm for T3 & T4 and 20 cm for T5 to T12, as represented in the Figure 2. The effective shear section of the wall is Si=L ti. The specimen includes short perpendicular walls (flanges) at both ends. The bottom and the top are made of a very rigid beam, with a negligible flexibility in the vertical plan.

In the design assumptions the conventional concrete capacity was f_{c28}^{d}=30 MPa. According to code specification (AFNOR 1992), and for a 0.2 Poisson's ratio, the conventional design shear modulus, G^{d}, was estimated at 14240 MPa and the design shear stiffness was given by the formula (1). K^{d}_{i} values and associated design eigenfrequencies, f^{d}_{i}, are reported in the Table 1, with the corresponding masses M_i (M1+M2 of the Figure 1). The design damping ratio was assumed as ξ^{d}=7%.

$K^{d}_{i}=G^{d}\ S_i\ /H$ = 5696 MN/m (i=3 and 4) or 7120 MN/m (i=5 to 12). (1)

For every specimen, the reinforcement to be implemented in the vertical and in the horizontal directions of the web was selected as indicated in the Table 1. The reinforcement is expressed in terms of density, ρ_h^{d} and ρ_v^{d}, which means the ratio of the steel section divided by the concrete section. The required reinforcing bar capacity was f_e^{d}=500 MPa. Reinforcement details are provided by Labbé et al. (2015).

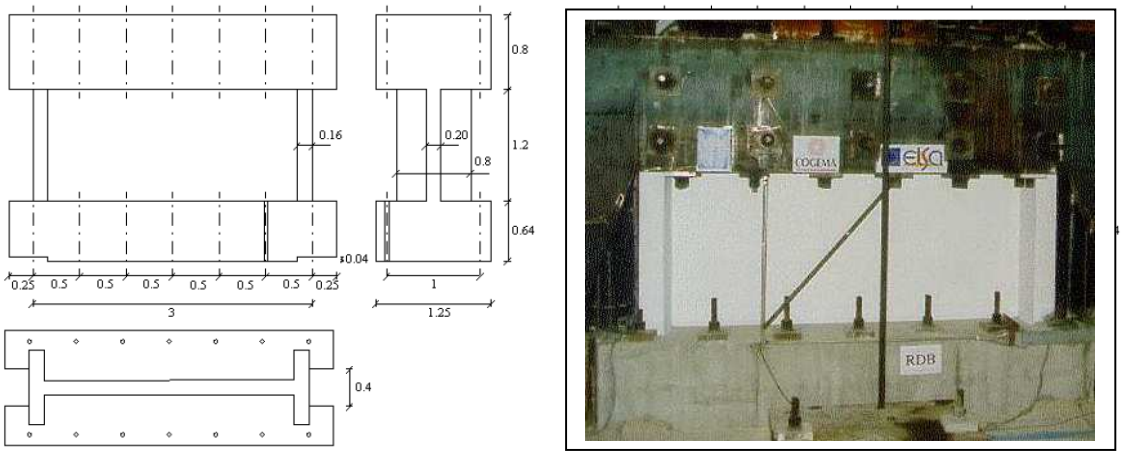

Figure 2. SAFE specimen geometry (Ti, i=5 to 12) and photo of T6

Table 1 - Main features of the SAFE specimens according to the conceptual design

i	t	S	K^d	f^d	M	$\rho_h{}^d$	$\rho_v{}^d$	τ^d	$\sigma_n{}^d$	H^d	u^d	$s_0(f^d,\xi^d)$	β
	m	m²	MN/m	Hz	ton	%	%	MPa	MPa	kN	mm	m/s²	
3	0.16	0.48	5696	4	9018	0.8	0.8	4	0	1920	0.34	2.55	0.084
4	0.16	0.48	5696	12	1002	0.8	0.8	4	0	1920	0.34	1.49	1.289
5	0.20	0.60	7120	8	2818	0.8	0.8	4	0	2400	0.34	2.01	0.424
6	0.20	0.60	7120	12	1252	0.6	0.4	3	1	1800	0.25	1.49	0.967
7	0.20	0.60	7120	4	11272	0.6	0.4	3	1	1800	0.25	2.55	0.063
8	0.20	0.60	7120	12	1252	0.4	0.4	2	0	1200	0.17	1.49	0.644
9	0.20	0.60	7120	4	11272	0.4	0.4	2	0	1200	0.17	2.55	0.042
10	0.20	0.60	7120	4	11272	0.6	0.6	3	0	1800	0.25	2.55	0.063
11	0.20	0.60	7120	4	11272	0.4	0.4	2	0	1200	0.17	2.55	0.042
12	0.20	0.60	7120	4	11272	0.11	0.11	1.44	1	864	0.12	2.55	0.030
$f_{c28}{}^d$=30 MPa, $f_e{}^d$=500 MPa												$s_0(f^d,\xi^d)$ and β are introduced in section 2.3	

A conventional design practice for shear walls in the nuclear industry is based on an acceptance criterion expressed in terms of shear stress. At the moment when SAFE was conceived, this practice was corresponding to a conventional building code criterion (AFNOR 1992) applicable in France: In a shear wall under a vertical compressive design stress $\sigma_n{}^d$, the conventional acceptable design shear stress, τ^d, is directly related to the reinforcement ratio by the formula (2). For the SAFE walls, the vertical load was deemed to be nil, except that for T6, T7 and T12 a vertical stress $\sigma_n{}^d$ = 1 MPa was prescribed. Corresponding values of τ^d_i are presented in the Table 1, as well as the associated design shear force $H^d_i = S_i\,\tau^d_i$ and design top displacement $u^d_i = H^d_i / K^d_i$.

$$\tau^d = \rho_v f_e{}^d + \sigma_n{}^d \qquad (2)$$

The actual concrete capacity of every specimen, $f_{c28}{}^a$, tested on 15 cm cubic samples, is presented in the Table 2. Prior to running the seismic tests, the actual eigenfrequency, f^a_i, of every specimen was measured by low level vibrations (performed by the pseudo-dynamic method) and the corresponding elastic stiffness, K^a_i, was derived. Values of f^a_i, K^a_i and K^a_i / K^d_i are presented in the Table 2. Interestingly,

the average value, 0.67, is very close to the 0.7 median value obtained by Sozen and Moehle (1993). The actual damping ratio, ξ^a_i, was concurrently measured and is also reported in the Table 2.

Table 2 - Observed main features of the SAFE specimens

i	$f_{c28}{}^a$	f^a	K^a	K^a/K^d	ξ^a	$\sigma_n{}^a$
	MPa	Hz	MN/m		%	MPa
3	36.6	2.77	2730	0.48		0.37
4	46.8	10.0	3830	0.70	3.7	0.37
5	38.6	6.69	4994	0.70	2.6	0.32
6	39.9	10.4	5348	0.75	3.7	1.01
7	43.8	3.58	5767	0.80	4.2	1.01
8	34.4	9.60	4557	0.64	4.1	0.32
9	43.0	2.91	3742	0.53	4.6	0.32
10	50.8	3.30	4846	0.68	2.2	0.32
11	44.9	3.30	4846	0.68	2.1	0.32
12	43.5	3.39	5144	0.72	3.0	1.01

2.3. Seismic input motions

The reference seismic input motion used in the SAFE programme is described by the response spectrum $s_0(f,\xi)$ presented in the Figure 3. An accelerogram $g_0(t)$ was derived, also presented in the Figure 3 with its response spectrum, which is reasonably close to $s_0(f,\xi)$.

Under $s_0(f,\xi)$, the conventional top relative displacement of the Ti specimen is calculated as $u^d_{0i}=s_0(f^d_i,\xi^d)/(2\pi\ f^d_i)^2$ and the corresponding conventional shear stress reads $\tau^d_{0i}=G^d\ u^d_{0i}/H$ (shear modulus times shear strain). Therefore, in order to get a shear stress that fits the above calculated conventional design τ^d_i, the reference input motion should be multiplied by the scaling factor $\beta_i = \tau^d_i / \tau^d_{0i}$:

$$g^d_i(t)=\beta_i\ g_0(t). \qquad (3)$$

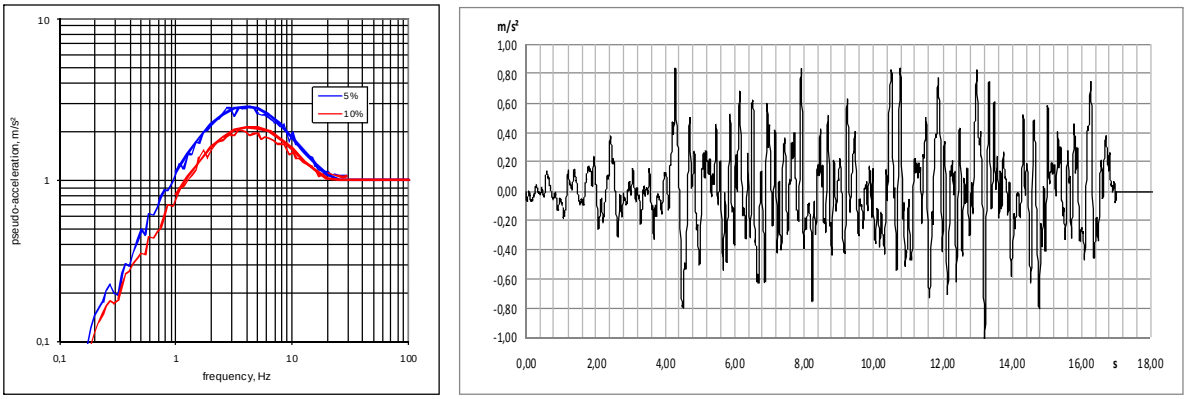

Figure 3 - Response spectra $s_0(f,\xi)$, and of $g_0(t)$ (left); Input motion $g_0(t)$ (right).

According to the nuclear industry practice, $g^d_i(t)$ is the design input motion for the specimen Ti. It means that $g^d_i(t)$ is a just acceptable input motion: for a larger input the calculated shear stress would exceed the acceptable one. Values of β_i are reported in the Table 1. Once $g^d_i(t)$ is determined, the test consists of a

series of runs of increasing levels, with input motions defined by the formula (4), in which α_{ij} is the amplification factor of the run j for the specimen Ti. For every specimen, the first run corresponds to α_{i1} =1. The α_{ij} values actually applied are reported in the Table 3.

$$G_{ij}(t) = \alpha_{ij}\, g^{d}_{i}(t). \quad (4)$$

The central frequency of $g_0(t)$, f_g = 4 Hz, is so that for T4, T5, T6 and T8 it is lower than the actual eigenfrequency of the specimen (low-frequency input) while for the other specimen it is the opposite.

3. Loading and monitoring systems

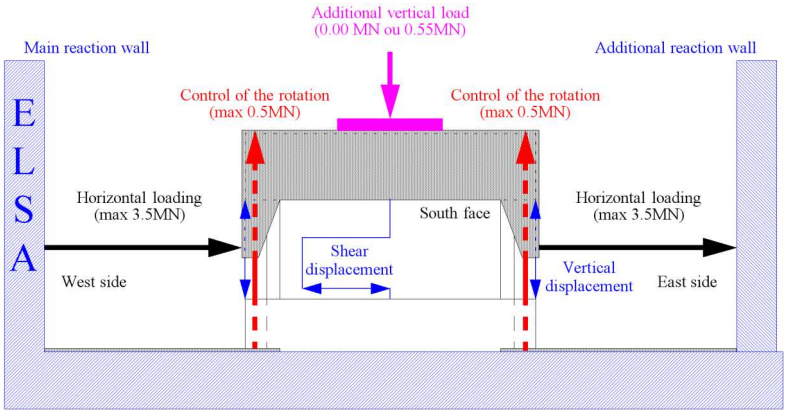

Figure 4 - Loading system

At its base, the specimen was clamped in the ELSA laboratory strong floor. At an end a horizontal force was applied by jacks attached on the ELSA reaction wall. At the other end, jacks were attached on an ad-hoc reaction device clamped in the strong floor. The loading system is presented in the Figure 4. A specific feature was that a rigid steel frame was fixed on the top beam, designed in such a way that the horizontal force was applied at the mid-height of the wall. Additionally two vertical jacks were implemented at the ends of the wall to control the top beam rotation and the total vertical load. The vertical displacements at the top of these two jacks were identical while the forces they apply were opposite (their sum vanished). For the specimen T6, T7 and T12, a complementary passive vertical load was centrally applied, increasing the vertical stress up to 1.0 MPa.

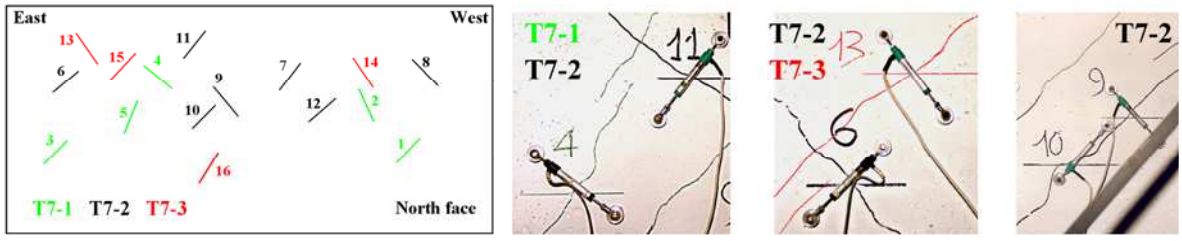

Figure 5 - Extra extensometers implemented on the specimen T7.

Forces applied by the horizontal and vertical jacks were monitored and the measures were used for the horizontal and vertical control. The horizontal differential displacement between the base and the top of the specimen was monitored and the measure was used for the control of the horizontal jacks. The vertical displacement between the base and the top of the specimen was also monitored at both ends and the measures were used for the control of the vertical jacks. A series of 32 extensometers was implemented. (See Labbé et al. 2015 for details)

An asset of the pseudo-dynamic method is that the test can be paused at any moment. For this reason an extra series of 16 short extensometers was available, to be implemented during the test, for crack opening monitoring. For instance, their T7 implementation is reported in the Figure 5 and six of them are visualized in the same figure. In this T7 case, five extensometers were implemented during the run 1, seven during the run 2 and the last four ones during the run 3.

4. Experimental outputs

4.1. Displacements and forces

A typical case of force-displacement records is presented in the Figure 6. The maximum observed top displacement u_{ij} and the maximum shear force H_{ij}, recorded during the run j of the specimen i, are reported in the Table 3. In particular u_{i1} and H_{i1} can be compared to u^d_i and H^d_i.

Consistently with the fact that the observed stiffness of the wall is significantly smaller than the calculated design stiffness, the recorded displacement is significantly larger than the calculated design displacement. This excess is more than a factor 10 for the stiff specimens (T4, T5, T6 and T8) and less than a factor 5 for the flexible ones.

Table 3 - Main outputs of the SAFE programme

i	j	α	u	H	w	f	ξ		i	j	α	u	H	w	f	ξ
			mm	kN	mm	Hz	%					mm	kN	mm	Hz	%
3	1	1	1.43	1635	0,3	1.7	6		8	1	1	2.56	2244	0,5	4.0	6
	2	2	4.64	2987	0,5	1.3	5			2	1.4	5.42	3289	0,9	3.3	6
	3	3	6.17	3484	1,0	1.1	6			3	1.8	11.85	3916	/	1.8	6
	4	5	11.7	3621	2,5	0.86	7		9	1	1	0.58	1052	0,2	2.3	6
4	1	1	8.06	4658	0,8	3.7	5			2	3	2.25	2362	0,4	1.5	6
	2	1.3	14.02	5302	1,2	2.3	6			3	6	5.74	3707	0,8	1.2	6
	3	1.5	27.02							4	10	15.8	4172	2,0	0.57	6
5	1	1	3.85	3523	0,4	2.7	5.5		10	1	1	0.78	1530	0,2	2.1	5
	2	1.3	6.50	4828	0,7	2.5	5.5			2	3	5.43	4352	0,7	1.3	6
	3	1.5	7.18	4934	0,7	2.4	5.5			3	6	11.57	5635	1,4	1.0	7.5
	4	2	10.3	5536	1,2	2.0	8			4	10	15.2	4925	3,5	0.75	10
6	1	1	3.10	2894	0,5	4.3	6		11	1	1	0.46	1179	0,2	2.4	4
	2	1.3	6.22	4282	0,8	3.5	6			2	6	6.47	3609	0,9	1.1	6
	3	1.5	8.79	4945	1,1	3.3	6			3	10	13.38	4096	2,3	0.75	10
	4	1.8	14.4	5180	1,8	2.4	10		12	1	1	0.25	1069	0,0	3.2	3
7	1	1	0.71	1815	0,2	2.4	6			2	3	0.85	1715	0,3	2.2	5
	2	2	1.86	2451	0,4	1.7	6			3	5	2.60	2462	0,7	1.5	6
	3	5	7.70	4921	1,1	1.2	6			4	10	7.8	3678	1,7	1.0	7
	4	10	20.0	5509	2,2	0.43	10			5	15	18.9	3818	2,7	0.51	10

i, j : specimen number, run number
α : amplification factor applied on the input $g^d(t)$ of the considered specimen
u, H, w : max. displacement, max. shear force, average max. crack opening recorded during the run
f, ξ : effective frequency and effective damping at the end of the run, derived from records. The precision on ξ is around 1%. A 5.5% value means that it was not possible to decide between 5% and 6%.

The recorded maximum shear capacity, H^{max}, exceeds significantly the design value, H^d. (H^{max} is the H value for the last run of the considered specimen in the Table 4; shear capacity excess ratio H^{max}/H^d is reported in the Table 4). This comes for a small part only from the fact that the actual concrete and steel capacities exceed the specified ones. Even when assuming the specified capacities for concrete and

steel (30 MPa and 500 MPa), pushover curves computed by Brun et al. (2011), show capacity excess by a factor of around 2, and even larger for the less reinforced walls.

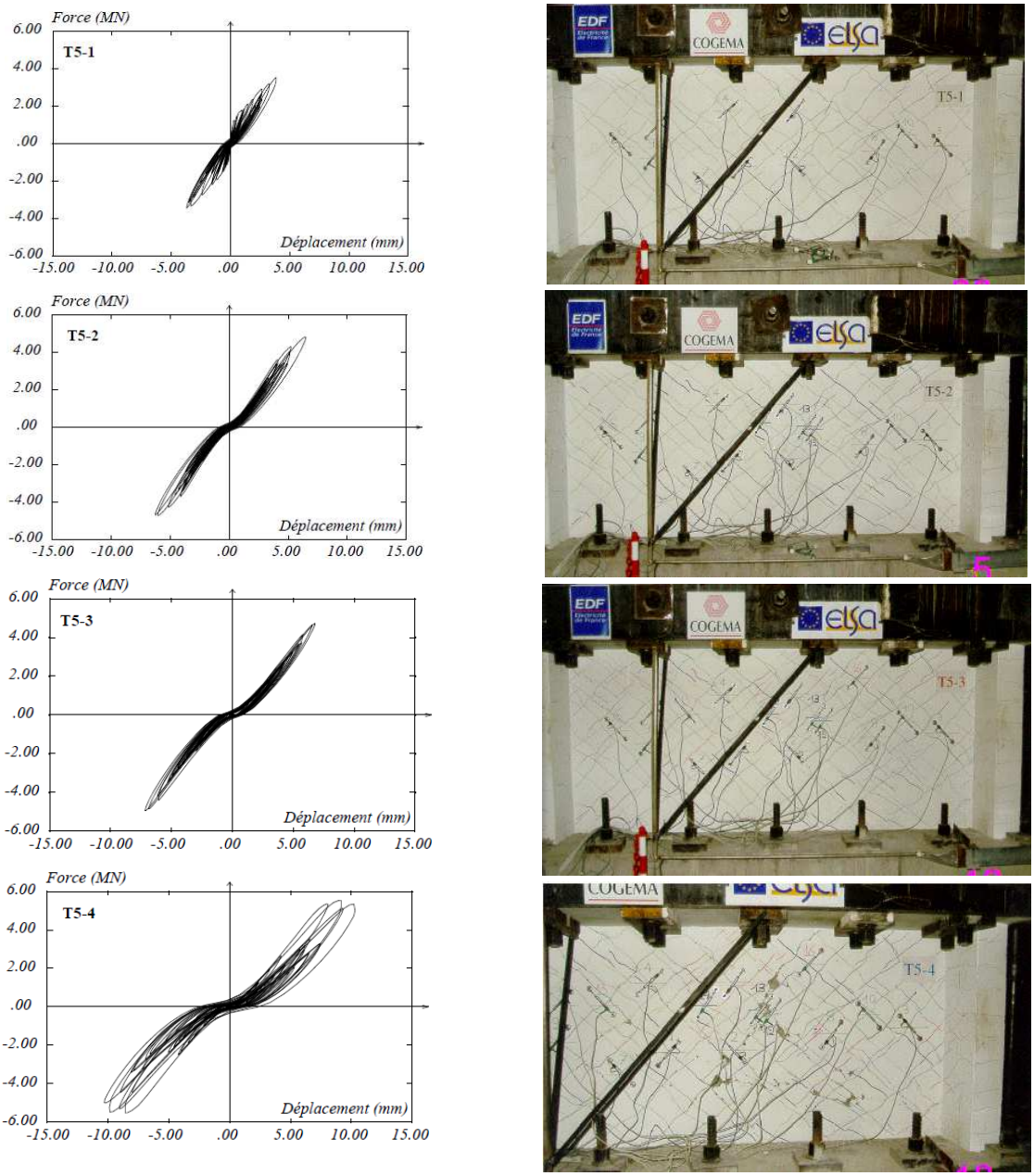

Figure 6 - Force-displacement records of T5 runs, Photos at the end of the runs

4.2. Empirical relationship between crack opening, drift and reinforcement

For every specimen Ti and every run j, a series of crack opening was recorded. Records were processed so as to derive the maximum opening, noticed w_{ij}., of the considered crack for the run j. For every run, the average maximum crack opening is presented in the Table 3. For instance, in the case of the wall T7, the value indicated in the Table 4 for the run 1 is the average of the 3 maximum crack opening values derived from the 3 extensometers that were implemented during this run. For the next runs, the reported value is the average derived from the crack opening extensometers operating during these runs.

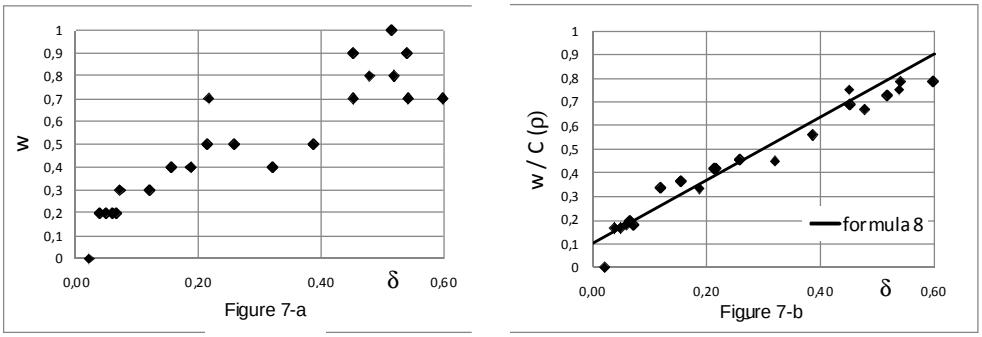

Figure 7-a Figure 7-b

Figure 7 - Crack opening (mm) versus drift (%): w raw data (left) and w/C(ρ) (right)

For every run, the observed drift, noticed Δ, is defined as the u value in the Table 4 divided by the specimen height, 1.2 m. Observed crack opening values are presented versus drift in the Figure 7-a. (the range of presented drift and crack opening is limited for the sake of clarity). Basically the crack opening is proportional to the drift. However experimental outputs provide evidence that the largest is the reinforcement density the lowest the crack opening for a given drift. This phenomenon is taken into account by the empirical formula (8), which minimizes the scattering that appears in the Figure 7-a (Labbé et al. 2015). In this formula w is in mm, Δ is in percent, ρ is the reinforcement density in percent, and C(ρ) is an empirical correcting coefficient. Values of w/C(ρ) versus Δ are plotted in the Figure 7-b. In this figure, C values are obtained through the formula (8b) from the ρ values that are presented in the Table 1 (for the specimens T6 and T7 the selected ρ value is 0.5).

$$w = (0.1 + 1.33\,\Delta)\,C(\rho), \quad \text{with} \quad C(\rho) = 0.2 + 0.9/(\rho + 0.5) \qquad (8a)\ \&\ (8b)$$

5. Types of seismic responses and margins

5.1. Categorization of specimen seismic responses

Similarly to α, which is a non-dimensional measure of input signals making them comparable in terms of anticipated damaging capacity, a non-dimensional measure of Δ is introduced in order to make responses comparable in terms of seismically induced damage. First Δ1 is calculated for every specimen as the drift corresponding to a 1 mm crack opening according to the Formula (8). (Values of Δ1 are reported in the Table 4). Then the reduced drift δ is introduced as:

$$\delta = \Delta/\Delta 1 \qquad (9)$$

Table 4 - Shear capacity excess. Drift and α values corresponding to a 1 mm crack opening

Specimen Ti	T3	T4	T5	T6	T7	T8	T9	T10	T11	T12
H^{max}/H^{d}	1.89	2.76	2.31	2.88	3.06	3.26	3.48	2.74	3.41	4.42
Δ1 (%)	0.77	0.77	0.77	0.61	0.61	0.55	0.55	0.66	0.55	0.37
α1	4.09	1.06	1.82	1.38	4.79	1.47	6.34	4.23	6.08	6.80

Values of δ versus α are plotted in the Figure 8. Two sets of outputs can be identified: the Set 1 of relatively flexible walls (f^{d}=4 Hz, 6 specimens) and the Set 2 of stiff walls (f^{d}=12 Hz, 3 specimens). The two sets exhibit an enormous difference regarding the sensitivity of the response to the level of input motion. For the Set 1, the response is practically proportional to the input level although the specimens are tested far in the non-linear regime. On the opposite, for the Set 2 the response exhibits a dramatic increase for a relatively small increase of the input beyond the design level. According to the analysis carried out by Labbé (2013), an interpretation of this phenomenon is that for the Set 1 the seismic input motion acts as a displacement controlled load whereas it acts as a force controlled load for the Set 2.

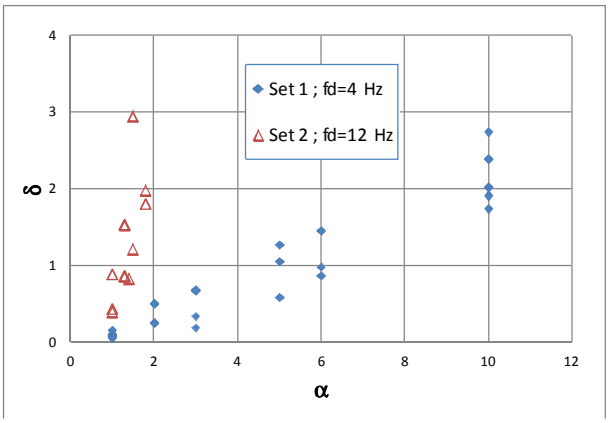

Figure 8 - Impact of specimen flexibility on the response to the seismic input level

In the SAFE experimental campaign, it was decided, for practical reasons relating to the conduct of the experiment, that a single input motion would be used and that consequently the experimental cases would be differentiated by the specimen eigenfrequency. However, it was already pointed out by Labbé and Noé (1992) and illustrated by Brun et al. (2003) that the key parameter is not exactly the natural frequency of the oscillator but the relative position of this frequency compared to the central frequency of the seismic input motion. We conclude that, when discussing the effects of beyond design seismic input motions, the expected frequency content of the input motion should be considered versus the structure natural frequency (or frequencies) because this relative frequency content has a dramatic effect on the seismic demand.

5.2. Seismic margins of SAFE specimens

In order to discuss margins a decision should first be made on the limit state that should not be exceeded under the design level earthquake. We assume here that this limit state is corresponding to a limited permanent deformation, which can be associated to a 1 mm crack opening. It means that the acceptable drift is $\Delta 1$, corresponding to a reduced drift $\delta=1$. On this basis the α value corresponding to the retained limit state, denoted $\alpha 1$, can be calculated for every specimen as presented in the Table 4. Then the average $\alpha 1$ values for Set 1 and Set 2 can be derived separately. The result, which can also be estimated from the Figure 8, is presented in the Table 5.

Table 5 - Design margins for relatively flexible walls (left) and relatively stiff walls (right)

	Set 1, f^d=4Hz	Set 2, f^d=12Hz
margin = average $\alpha 1$	5.4	1.3

This result means that, for the considered limit state, the design process provides a significant margin, by a factor of 5, for the Set 1 (relatively flexible walls) while this margin is limited to only 30 % for the Set 2 (stiff walls). This frequency dependence of the margin was already pointed out by Newmark (NRC 1978) when he introduced the inelastic response spectrum. Actually the inelastic response spectrum reflects the fact that for low frequency oscillators the margin is equal to the ductile capacity, whereas it tends to be equal to 1 for high frequency oscillators.

Note that the identified margin has little to do with the shear capacity excess H^{max}/H^d, discussed in section 4.1. For instance, except their frequency, the specimens T6 and T7 are identical and actually their capacity excess is similar, 2.88 for T6 and 3.06 for T7. However their margin is very different: 1.38 for T6 and 4.79 for T7. It means that for a Set 2 item like T6 the benefit of the capacity excess is partly counterbalanced by a detrimental dynamic effect. On the opposite, a Set 1 item like T7 benefits of a favourable dynamic effect.

Although the terminology of margin, at least in the sense adopted here, was not used by Newmark (NRC 1978), Iwan (1980) or Fajfar (1999), these authors investigated by numerical simulations the frequency dependence of structural seismic response. A major contribution of the SAFE research programme is to provide an experimental evidence of this frequency dependence phenomenon, summarized in the Figure 8, and to make experimentally explicit the corresponding design margins.

6. References

AFNOR (1992), Association Française de Normalisation, "Règles techniques de conception et de calcul des ouvrages et constructions en béton armé suivant la méthode des états limites", DTU P18-702.

Brun, M., Reynouard, J.M., Jézéquel, L., (2003). "A simple shear wall model taking into account stiffness degradation", *Eng. Struct. 25, 1–9.*

Brun, M., Labbé, P., Bertrand, D., Courtois, A., (2011). "Pseudo-dynamic tests on low-rise shear walls and simplified model based on the structural frequency drift", *Eng. Struct. 33, 796–812*.

Fajfar P. (1999), "Capacity spectrum based on inelastic demand spectra", *Earthquake Engineering and Structural Dynamics, Vol. 28, 979-993*

Gallitre E. (2008), "Fissuration des voiles courts en béton armé soumis à des solicitations sismiques, evaluation des ouvertures de fissures", PhD, Institut National des Sciences Appliquées, Lyon.

Gallois Ch. (1994), "Programme de recherche sur le comportement sismique de structures armées faiblement élancées" (Programme SAFE), SGN Internal report 94/354/000/154, 20-12-1994

Grammatikou S, Biskinis D, Fardis M.N. (2014), "Strength, deformation capacity and failure mode of RC walls in cyclic loading", *4th International fib Congress and Exhibition, 408*, Mumbai, India

Gulec C. K., Whitakker A.S. (2009), "Performance based assessment and design of squat reinforced concrete shear walls", *Technical Report MCEER-09-0010,* State Univ. Of New York, Buffalo, NY.

IAEA (2011), "Non-linear Response to a Type of Seismic Input Motion", *TECDOC 1655,* International Atomic Energy Agency, Vienna.

Iwan W.D. (1980), "Estimating inelastic response spectra from elastic spectra", *Earthquake Engineering and Structural Dynamics, Vol. 8, 375-388*

Kitada, Y., Nishikawa, T., Takiguchi, K., Maekawa, K., (2006) "Ultimate strength of reinforced concrete shear walls under multi-axes seismic loads", *Nucl. Eng. & Design*

Kotronis P., Mazars J., Davenne L. (2003), "The equivalent reinforced concrete model for simulating the behavior of walls under dynamic shear loading", *Engineering Fracture Mechanics 70 1085–1097*.

Labbé P., Noé H. (1992), "Ductility and Seismic Design Criteria", *Proceedings of the 10th World Conference on Earthquake Engineering, Madrid*, Brookfield, Rotterdam.

Labbé P. (2013), "Categorization of seismically-induced stresses for civil and mechanical engineering", *Nuclear Engineering and Design 255, 240– 247*

Labbé P. Pégon P., Molina F.J., Gallois Ch., Chauvel D.(2015), "the SAFE experimental research on the frequency dependence of shear wall seismic design margins", *under printing Journal of Earthquake Engineering,* Taylor & Francis.

Mazars J. Kotronis P., Davenne L., (2002) "A new modelling strategy for the behaviour of shear walls under dynamic loading", *Earthquake Engng Struct. Dyn. 2002; 31:937–954*

Molina F.J., Magonette G., Pegon P., Zapico B. (2011), "Monitoring Damping in Pseudo-Dynamic Tests", *Journal of Earthquake Engineering, 15:6, 877-900*

NRC (1978), "Development of Criteria for Seismic Review of Selected Nuclear Power Plants", *NUREG/CR-0098, Nuclear Regulatory Commission,* Washington, DC.

NRC (1994), "Technical Guidelines for Aseismic Design of Nuclear Power Plants" – Translation of JEAG 4601-1987, *NUREG/CR-6241 BNL-NUREG-52422, Nuc. Reg. Commission, Washington, DC.*

Pégon P. (1999), "Programme SAFE, Présentation générale des essais", *in Réévaluation sismique du genie civil des installations nucléaires, Journée Technique SFEN-ST9, 14-12-1999,* Paris.

Pégon P., Molina F.J., Magonette G. (2008), "Continuous pseudo-dynamic testing at ELSA", *in Hybrid Simulation; Theory, Implementation and Applications, 79-88,* Taylor & Francis/Balkema Publishers.

Sozen M.A., Moehle J.P. (1993), "Stiffness of Reinforced Concrete Walls Resisting In Plane Shear", *Report No. EPRI TR-102731* Electric Power Research Inst., Palo Alto (CA).